The self-associating behavior of NH_3 and ND_3 in liquid xenon

Accepted Manuscript

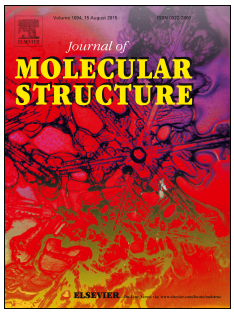

The self-associating behavior of NH_3 and ND_3 in liquid xenon

Liene I. De Beuckeleer, Wouter A. Herrebout

PII: S0022-2860(16)30297-6

DOI: 10.1016/j.molstruc.2016.03.089

Reference: MOLSTR 22400

To appear in: *Journal of Molecular Structure*

Received Date: 7 December 2015

Accepted Date: 25 March 2016

Please cite this article as: L.I. De Beuckeleer, W.A. Herrebout, The self-associating behavior of NH_3 and ND_3 in liquid xenon, *Journal of Molecular Structure* (2016), doi: 10.1016/j.molstruc.2016.03.089.

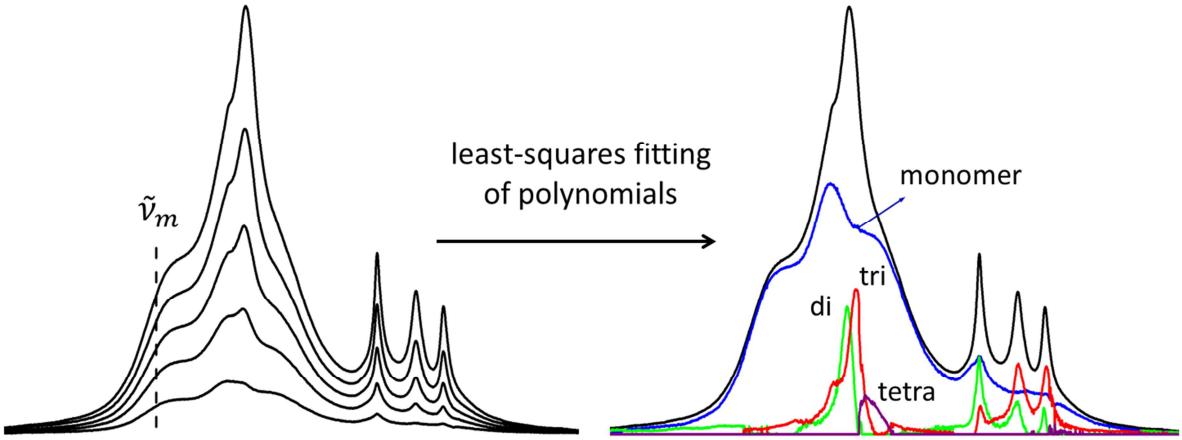

The self-associating behavior of NH_3 and ND_3 in liquid xenon

Liene I. De Beuckeleer, Wouter A. Herrebout*

*Department of Chemistry, University of Antwerp, Groenenborgerlaan 171, 2020 Antwerp, Belgium

Keywords

Ammonia, Ammonia-d_3, self-association, cryosolutions, liquid xenon, infrared spectroscopy, least-squares fitting, monomer, dimer, trimer, tetramer

Abstract

In this study we report on the analysis of isothermal spectra of NH_3 and ND_3 solutions in liquid xenon at 203 K using newly developed and validated least-squares approaches to investigate the its self-associating behavior. For both species we observe clear dimer bands in the spectral area of the $\nu_1+\nu_4$, $\nu_3+\nu_4$ and $\nu_1+\nu_2$, $\nu_3+\nu_2$ combination bands. The analysis of the N–D stretching area, allows us to characterize clear contributions of dimers and trimers. The analysis of the N–H stretching area is hampered by the occurrence of a time dependent band due to solid water traces during the experiments. For NH_3 we also performed an investigation of the N–H bending region, ν_2, which demonstrated a small dimer absorption band. These obtained results compare well with literature data.

* wouter.herrebout@uantwerpen.be

1. INTRODUCTION

Solutions in liquefied inert gases have proven to be an ideal medium to study molecular complexes held together by weak and medium-strong interactions.[1] They create a weakly interacting environment that, combined with the low temperatures used, leads to small bandwidths and thus facilitates the detection of complex bands only slightly shifted from the monomer modes. Although most experiments reported are focusing on heterocomplexes involving an electron rich Lewis base and an electron deficient region related to a hydrogen bond [2-4], a halogen bond [4-7] or a lone pair-π acceptor [8], these solutions also form an ideal medium to investigate self-association through hydrogen bonding between two, three or more identical molecules.

Information on the appearance of self-association in the cryosolutions studies is typically obtained from isothermal experiments, in which spectra of solutions containing different concentrations of the solute are recorded. In many cases, the contributions of the monomer and the oligomeric species are approximated by subtracting the spectra of solutions containing larger amounts of the solute and a rescaled spectrum of a highly diluted solution recorded under similar circumstances. Subsequently, information on the origin of the different features observed in the difference spectra is obtained by determining their integrated intensities and their dependence upon the monomer intensity. This subtraction approach is somewhat limited as it requires that at the lowest concentrations studied the contribution of complex species in the spectra is negligibly small. Moreover, because the outcome of least-squares band fitting procedures used to determine the integrated intensities of the different spectral features often depends strongly on the initial parameters chosen and thus can be biased by the end-user, integrated intensities obtained for the different species often are less reliable than required.

To overcome these problems, we have recently reported on the development and validation of numerical methods in which the concentration dependent behavior observed for HCl in liquid argon is analyzed by least-squares fitting approaches. [9] In these methods, for each wavenumber a polynomial is used to mimic the relation between monomer concentrations and measured absorbances. It was shown that by selecting the appropriate polynomial degree by using the *BIC* selection criterion, and by introducing additional constraints prohibiting negative absorbances to occur for the monomer and oligomers, the contributions due to monomers and self-associated

species can be determined with a much higher accuracy than before. To further validate the models developed, in this study, results obtained for solutions of ammonia (NH_3) dissolved in liquid xenon (LXe), for which similar but more complicated spectral features due to self-association are known to exist [10,11], are reported. It is important to stress that, although spectral features due to self-association have been observed for ammonia in LXe, the data obtained for NH_3 [10,11] did not allow a detailed assignment of the features observed. Moreover, for ND_3, no such studies were yet reported.

By combining new experimental data and the recently developed methodologies we aim to i) to further expand and analyze the available data for ammonia, and ii) to complement the data available with data derived for ND_3. The results will also be compared with literature data focusing on the earlier observations of different types of clusters in solid matrices.

2. EXPERIMENTAL SECTION

NH_3 (stated purity of 99,99%) and ND_3 (stated purity of 99%) were purchased from Sigma-Aldrich and Cambridge Isotope Laboratories respectively and were used without further purification. The xenon used as a cryosolvent had a stated purity of 99.999% and was supplied by Linde.

A dataset of 328 infrared spectra for NH_3 and 246 spectra for ND_3 solutions in LXe was recorded on a Bruker IFS 66v Fourier transform spectrometer. A Globar source was used in combination with a Ge/KBr beamsplitter and a LN_2-cooled broad band MCT detector. The interferograms were averaged over 500 scans at an unapodized resolution of 0.5 cm^{-1}, averaged over 500 scans, and Blackman–Harris three-term apodized before Fourier transformation. The experimental set-up used to investigate the solutions in liquid noble gases has been described before.[1] In the actual cryostat, a liquid cell with 1 cm path length, equipped with wedged Si windows was mounted below a LN_2 Dewar. The temperature of the cell body is measured using a Pt-100 thermoresistor. The SunRod electric minicartridge heater is controlled using a Eurotherm 3504 PID controller. The temperature of the solutions was stabilized at 203 K, the temperature variation during a typical run being less than 0.05 K. Spectra were obtained and pre-analyzed using OPUS 6.5. Further analyses were performed using Matlab.[12]

The mole fractions of NH_3 and ND_3 used for the datasets are difficult to accurately quantify[13,14], but are estimated to vary between 1.5×10^{-2} and 9.4×10^{-4} for NH_3 and 9.4×10^{-3} and 9.4×10^{-4} for ND_3. The concentrations used are chosen so that the region between minimum and maximum absorbance is uniformly covered.

As the outcome of the used fitting procedures can be strongly influenced by baseline artefacts, it was found necessary to perform baseline corrections on the complete dataset using spectra of pure LXe recorded at exactly the same conditions. Another critical parameter often hampering the numerical analyses to be performed is related to small traces of solid, amorphous or crystalline water suspended in the solution or condensed onto the cold elements present in the cryostat and/or detector. As is clear from the bottom panel in Figure 1, these water traces manifest themselves as a broad band in the 3650-3050 cm^{-1} region which fully overlaps with the N–H stretching region of NH_3 and with a combination band of ND_3. The traces are observed to slightly increase during experiments, and, due to changes in relative intensities, are extremely difficult to subtract. Therefore, to avoid further numerical instabilities, no such corrections were introduced. To account for remaining baseline drifts, which we believe are due to small temperature changes inside the spectrometer due to the colder parts present, additional straight line baseline corrections was applied to all data. For NH_3 these straight lines were generated from 6850 to 6210, from 6210 to 5620, from 5620 to 3990, from 3990 to 2205, and from 2205 to and 665 cm^{-1}. For ND_3 these lines were generated from 5365 to 5023, from 5023 to 4362, from 4362 to 3390, from 3390 to 3005, from 3005 to 1820, and from 1820 to 535 cm^{-1}.

3. RESULTS AND DISCUSSION

3.1 Least-squares fitting method: general concept

Recently, a least-squares based methodology to isolate overlapping absorption bands of monomeric and oligomeric species observed in the spectra of cryosolutions was developed and validated.[9] The method is based on the assumption that the measured absorbance at a wavenumber $\tilde{\nu}_i$, $A_{exp}(\tilde{\nu}_i)$ is the sum of individual contributions related to the monomer, A_{mono}or to one of the oligomers, e.g. dimer A_{di}, trimer A_{tri}, tetramer A_{tetra}, etc., i.e.

$$A_{exp}(\tilde{\nu}_i) = A_{mono}(\tilde{\nu}_i) + A_{di}(\tilde{\nu}_i) + A_{tri}(\tilde{\nu}_i) + A_{tetra}(\tilde{\nu}_i) + \cdots \quad (1)$$

The experimental absorbances for each wavenumber $\tilde{\nu}_i$ of all contributing species in the solution are then expressed as a function of the absorbance of a chosen monomer wavenumber $\tilde{\nu}_m$ with the polynomial degree p equal to 1, 2, 3, 4 or 5 with intercept equal to zero

$$A_{exp}(\tilde{\nu}_i) = \sum_{p=1}^{n} a_{\mathrm{p}}(\tilde{\nu}_i, \tilde{\nu}_m)\,[A_{mono}(\tilde{\nu}_m)]^p. \tag{2}$$

the coefficient $a_{\mathrm{p}}(\tilde{\nu}_i, \tilde{\nu}_m)$ being a constant related to the equilibrium constant of the oligomerization reaction.[9] The monomer wavenumber $\tilde{\nu}_m$ is used as an internal standard and is chosen based on the fact that no features due to self-association are observed or expected to appear in the region considered. Moreover, special attention is paid to the fact that for all concentrations studied the absorbance can be accurately determined. When there is no change in the measured absorbance with increasing monomer concentration, a 0^{th} degree polynomial or constant is the best model to mimic this relation.

In the applied model selection procedure, the experimental data for a given wavenumber are least-squares fitted using a series of polynomials of 1^{st}, 2^{nd}, 3^{rd}, 4^{th} and 5^{th} degree. Subsequently, the 'better' polynomial model is selected with the B information criterion, *BIC*, published by Schwarz [15] and defined as

$$BIC_p(\tilde{\nu}_i) = \mathrm{n} \cdot \ln\left(\frac{RSS_p(\tilde{\nu}_i)}{n}\right) + k \cdot \ln(n) \tag{3}$$

with n as the number of spectra in the dataset which is equal to the number of measured datapoints for each wavenumber and k as the number of fitted parameters and with sum of squares *RSS*, defined as

$$RSS_p(\tilde{\nu}_i) = \sum_{k=1}^{n} [A_{exp,k}(\tilde{\nu}_i) - A_{calc,k}\,(\tilde{\nu}_i)]^2 \tag{4}$$

Here, we define the "better" model as the model that is parsimonious in the polynomial degree *p* and one that has a smaller residual sum of squares, *RSS*

Despite the model selection strategy, higher degree polynomials lead to compensation effects in which a large positive contribution is calculated for one of the species, and another strongly negative compensating feature is predicted for another. To avoid this kind of noise, nonnegative constraints were added, prohibiting the coefficients to become negative during the polynomial regression.

In the following paragraph the recorded dataset will be analyzed by fitting a series polynomials with nonnegative constraints through the measured absorbance values for every wavenumber individually. The data for the different wavenumbers thus are completely independent. After selection of the appropriate polynomial degree using the *BIC*, the contributions for every wavenumber are calculated and combined and the isolated spectra of the species present in the solution are obtained without further smoothing.

It should also be noted that when showing the results a value will be shown for the constant until pentamer contribution. If the selected degree does not allow a certain contribution the coefficient will be set to be zero resulting in a contribution equal to zero.

3.2 The NH_3 and ND_3 spectra and subtraction procedures

Figure 1 shows typical infrared spectra from the database of NH_3 and ND_3 recorded at 203 K with liquefied xenon as solvent. The broad absorptions with substantial PQR structure observed in the N–H stretching region, 3950-3000 cm^{-1}, and the N–D stretching region, 2800-2200 cm^{-1}, are caused by the overlapping ν_3 (degenerate asymmetric stretching vibration), ν_1 (symmetric stretching vibration) and $2\nu_4$ (overtone of asymmetric bending vibration) monomer bands, of which the band centers and relative intensities are difficult to determine.[3,11] The inserts given in Figure 1 illustrate that with increasing concentration of NH_3 or ND_3, new bands due to self-associated species emerge.

The fundamental vibrations ν_4 (degenerate asymmetric bending vibration) and ν_2 (symmetric bending or umbrella vibration) are observed near 1618 and 960 cm^{-1} for NH_3 and 1183 and 770 cm^{-1} for ND_3. As before, rotational PQR structure due to hindered internal rotation of ammonia in the cryosolutions is observed for all modes. It is clear from Figure 1 that, whereas features due to self-associating are easily observed for the stretching regions, no such features can be deduced for the other modes. The different behavior is explained by the fact that upon complexation, an extreme increase in infrared intensity, by a factor up to 80 times [16] is observed for the N–H and N–D stretching modes, whereas the intensity of the other modes is hardly influenced. From this, it must be concluded that, although features due to self-association are clearly visible in some regions of the spectra, their equilibrium concentration in the solutions studied should still be remarkably low. Apart from the band ascribed above, in the spectra of NH_3

and ND_3, additional bands are observed near 5026 and 4415 cm^{-1} and 3724 and 3321 cm^{-1}, respectively. These bands are assigned to the combination $\nu_1+\nu_4$, $\nu_3+\nu_4$ and $\nu_1+\nu_2$, $\nu_3+\nu_2$ respectively.[11] The feature at 4865 cm^{-1} observed in the spectra of ND_3 originates from the $\nu_1+\nu_3$ combination. The absorption near 1455 cm^{-1} observed in the spectra of ND_3 is assigned to a trace of ND_2H present in the ND_3 sample used. Based on calculated infrared intensities for both samples, and on existing literature data [17], the relative abundance of this species in the solution is estimated to be close to 6 %. It may be noted that, due to severe overlap with modes of the parent molecule, no features due to ND_2H were observed for other spectral regions. Also, no features due to NDH_2 were detected.

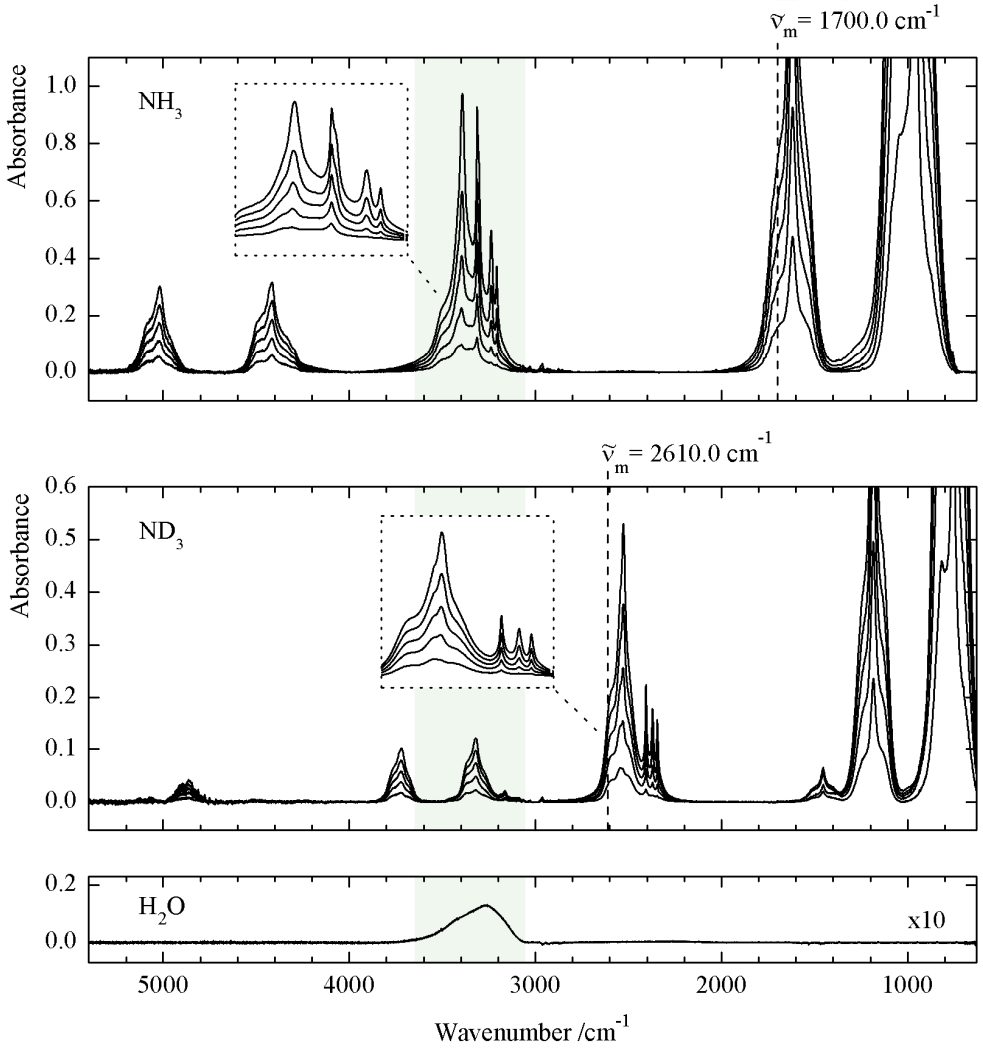

Figure 1. Infrared spectra of solutions in LXe at 203 K, with at the top 5 spectra of NH_3 and at the middle 5 spectra of ND_3. The spectra shown for each of the species represent only a small fraction of the spectral database

used in the fitting procedures. The N–H and N–D stretching areas are magnified in the inserts. The bottom spectrum is an example of a spectrum of solid water that builds up during the measurements. Its spectral region is illustrated by the shaded area.

As a benchmark for least-squares polynomial fitting approaches, it is helpful to analyze the results that can be obtained using standard subtraction procedures. As mentioned before, these approaches are based on the assumption that at the lowest concentrations studied, only absorptions due to monomeric species are present. Moreover, it is assumed that in the concentration range studied the monomer spectrum does not change. The subtraction procedure also requires the scaling factor of the diluted spectrum to be optimized. To this end, we have chosen to compare the absorbances at the reference wavenumbers $\tilde{\nu}_m$ = 1700.0 cm^{-1} for NH_3 and $\tilde{\nu}_m$ = 2610.0 cm^{-1} for ND_3. For completeness, the used reference wavenumbers $\tilde{\nu}_m$ are denoted with a dashed line in Figure 1.

The resulting spectra for $(NH_3)_x$ and $(ND_3)_x$ obtained from the subtraction procedures based on the reference wavenumbers given and based on the spectra given in Figure 1 are shown in the top panels of Figure 2. The spectral analysis for the 2330-500 cm^{-1} spectral region, obtained for solutions that, due to the strong infrared intensity of the monomer band, are diluted by a factor of approximately 5 are given in the lower panel. In agreement with the above observations, intense oligomer features, shown in trace c, are observed in the N–H and N–D stretching areas. In addition, weaker features not immediately obvious from Figure 2 are also present in the regions of the combination bands and of the NH_3 bending mode ν_2.

It should be stressed that because of the underlying nature, the subtraction procedures described above allow estimating the total spectrum of the self-associated species, but do not allow the accurate determination the individual contributions due to the different species present. A more thorough analysis of the spectral data available therefore requires more rigorous approaches including, e.g. the least-squares fitting methodology recently developed.

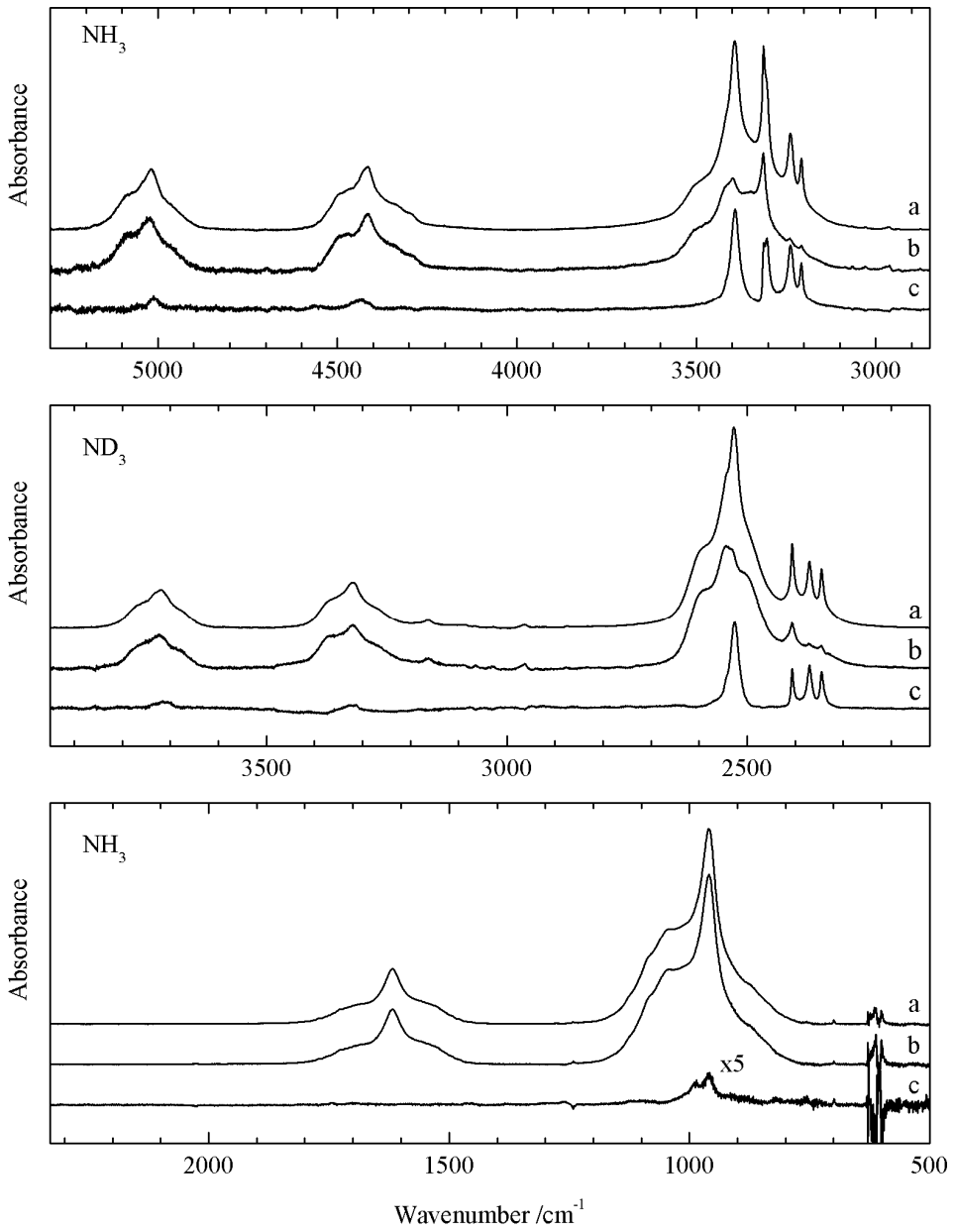

Figure 2 Subtraction procedure involving an original spectrum of a concentrated solution of NH_3 and ND_3 in LXe, trace a, and a rescaled spectrum of a highly diluted solution recorded under the same conditions, trace b. The result of the subtraction showing the summed contributions of the different oligomers present is given in trace c.

3.3 Separating monomer and oligomer contributions

Figure 3A and 3B show the results obtained by using polynomial regression with added nonnegative constraints, using the minimum value of the *BIC* to select the appropriate polynomial degree for every wavenumber. The selection is made between polynomials of 0^{th} to 5^{th} degrees, allowing all contributions up to pentamer to be included. Comparison of the results based on the least-squares fitting procedure and those derived from the subtraction procedures shows that, in general results are comparable. However, more detailed information about the origin of the oligomeric features can be obtained with the numerical methods.

The N–H stretch has been shown to be most sensitive to the formation of N–H···N hydrogen bonded clusters and this region was studied.[16] The presence of the changing water band around 3500-3100 cm^{-1} prevents a reliable fitting of the polynomials in the N–H stretching region. The results shown in Figure 3A assign the found oligomer features only to dimers and pentamers and not to trimers and tetramers. This seems very unlikely and does not compare with the results from earlier observations in solid matrices and liquid helium droplets, illustrated in Table 1. Furthermore, these features are also not compatible with the results for ND_3, which are discussed in the next paragraph.

As the water band does not overlap with the ND_3 stretching regions and analysis allows contributions due to dimer and trimer species to be reliably characterized. The absorption bands are resolved in dimer contributions at 2529, 2406, 2370 and 2346 cm^{-1} and trimer features at 2541, 2519, 2369 and 2343 cm^{-1}. Moreover, a feature due to a tetramer is calculated to appear near 2507 cm^{-1}. Inspection of the data obtained with limited literature data summarized in Table 2 shows that for both the dimer and the trimer, good agreement is observed between the wavenumbers derived from the cryosolutions and those derived from the solid argon matrices by Süzer and Andrews[18].

As illustrated in Figure 3A and 3B, for the combination bands $\nu_1+\nu_4$, $\nu_3+\nu_4$ and $\nu_1+\nu_2$, $\nu_3+\nu_2$ for NH_3 and for ND_3 absorption bands can be assigned to dimers. Apart from these features, additional, weaker traces due to a trimer are also present in three of the regions. Unfortunately, the limited signal-to-noise ratio due to low intensities and, consequently, low absorbances, make an unambiguous assignment of these trimer bands impossible.

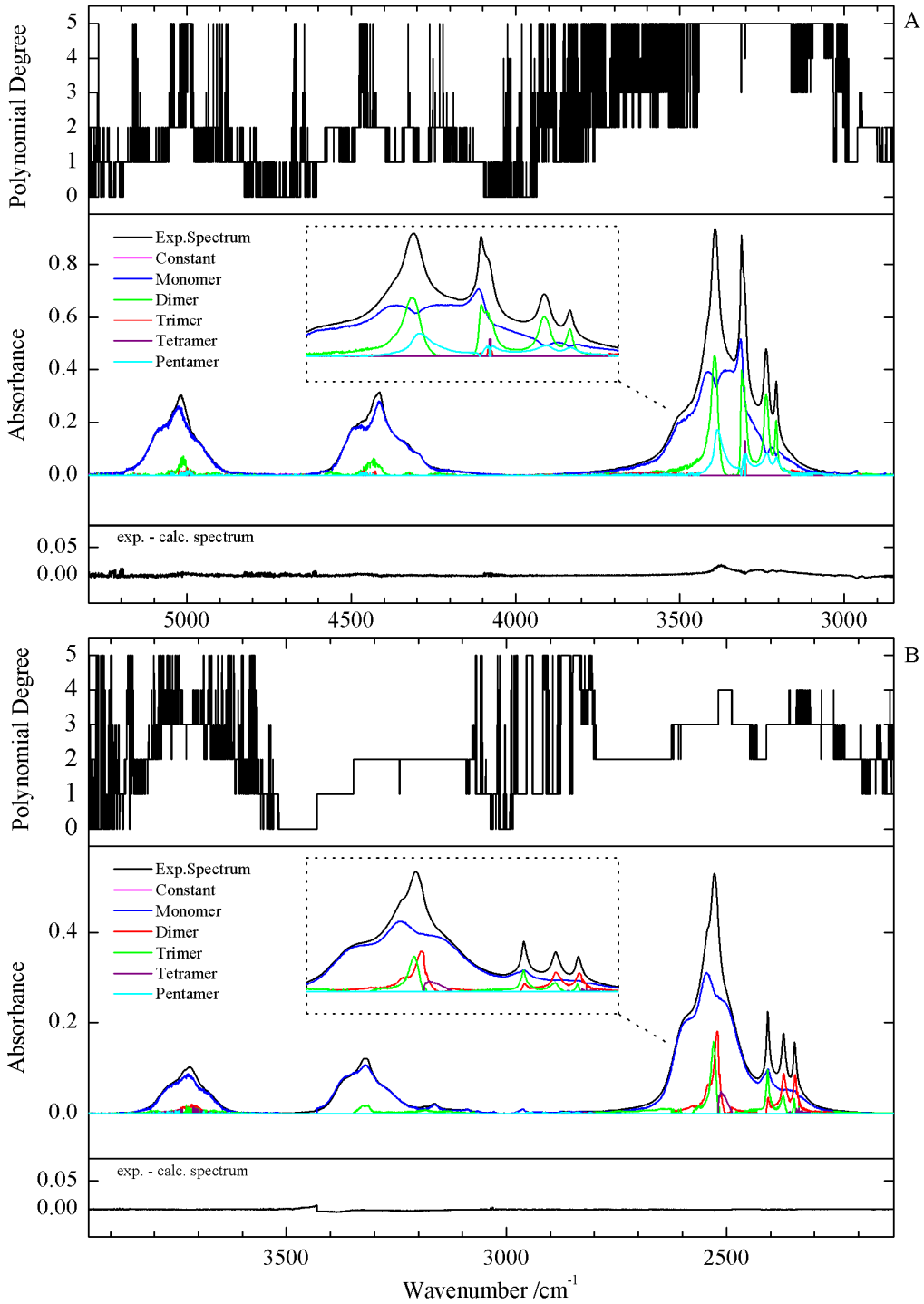

Figure 3 The results for the 5300-2850 cm^{-1} region of NH_3 (A) and the 3950-2100 cm^{-1} region of ND_3 (B) obtained by analyzing the experimental data with polynomial regression with added nonnegative constraints, using the minimum value the *BIC* to select the appropriate polynomial degree varying between

0 and 5 for every wavenumber. The bottom panel shows the difference between the experimental and calculated spectrum. The N–H and N–D stretching areas are magnified in the insert.

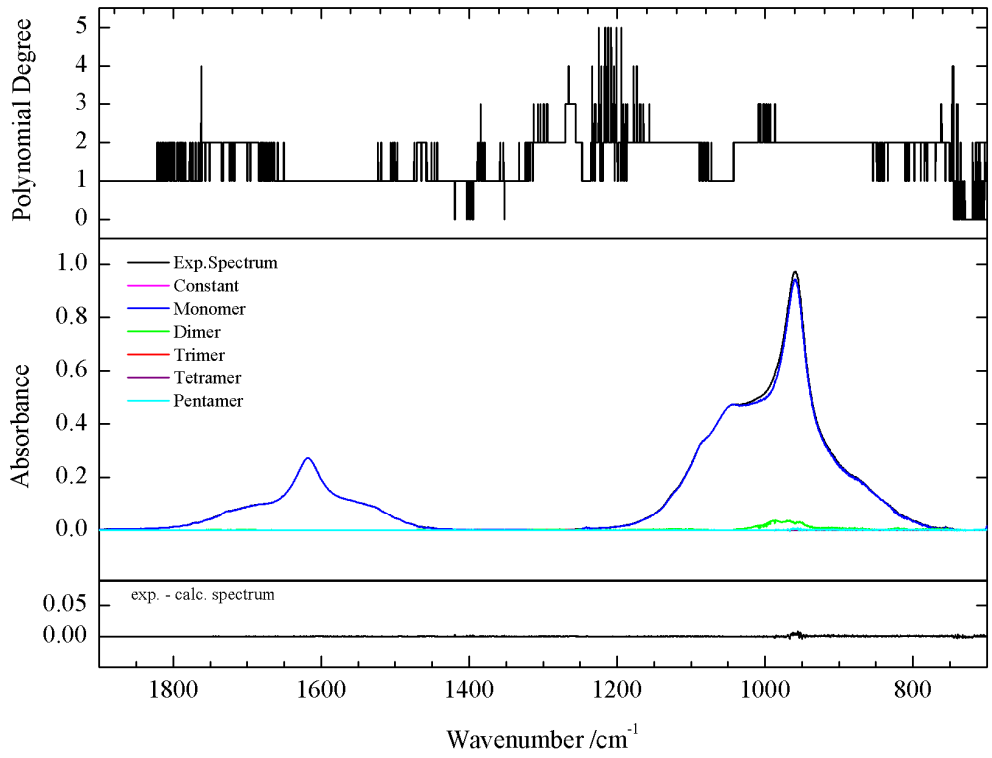

Figure 4 The results for the 1900-775 cm^{-1} region of NH_3 obtained by analyzing the experimental data with polynomial regression with added nonnegative constraints, using the minimum value the *BIC* to select the appropriate polynomial degree varying between 0 and 5 for every wavenumber. The bottom panel shows the difference between the experimental and calculated spectrum.

Figure 4 summarizes the results for the NH_3 bending vibration ν_2. The indicated results were obtained using a spectral database of only 85 spectra, i.e. using a database significantly smaller than that used for the other regions. The reason for this is related to the strong infrared intensity which, in combination with the characteristics of the MCT detector and the optical path length of 10 mm used do not allow accurate intensities to be measured for larger concentrations. Inspection of the data in Figure 4 clearly shows that in this spectral region, the measured spectra are largely dominated by the monomer contributions with origins at 1618 and 960 cm^{-1} for ν_4 and ν_2, the only feature illustrating the presence of higher associations being a weak dimer band around 970 cm^{-1}. The observed complex band derived from the polynomial regression using *BIC*

selection matches quite well with that derived from the subtraction procedures. As illustrated in Table 1 the observed complexation shift is in line with the shifts reported by Süzer and Andrews.[18]

4. CONCLUSIONS

In this study we report on the analysis of isothermal spectra of NH_3 and ND_3 solutions in LXe using the newly developed and validated least-squares fitting of polynomials methodology. For both species we observe clear dimer bands in the spectral area of the $\nu_1+\nu_4$, $\nu_3+\nu_4$ and $\nu_1+\nu_2$, $\nu_3+\nu_2$ combination bands. There are also some weaker trimer signals but because of the limited signal-to-noise ratio due to low intensities and, consequently, low absorbances, it is impossible to make an unambiguous assignment. The analysis of N–D stretching area allowed us to characterize clear contributions of dimers and trimers. For NH_3 we also performed an investigation of the N–H bending region which demonstrated a small dimer absorption band.

In general the analyses are hampered by the occurrence of a time dependent band of solid water traces which was impossible to subtract as it overlaps with the N–H stretching region for NH_3 and the $\nu_1+\nu_2$, $\nu_3+\nu_2$ for ND_3. Therefore it was not possible to determine a reliable assignment for the oligomer signals in the N–H stretching region. The obtained results are in good comparison with literature data on ammonia clusters in solid matrices.

TABLES

Table 1. Assignment of the monomer and resulting oligomer absorption bands of NH_3 in LXe at 203 K and a comparison with previous literature investigations.

Assignment	Experiment	Literature							
	Liquid Xe 203 K	Liquid Xe [11] 178K	Ar matrix[18]	Ar matrix[19]	Ar matrix[20]	Ne matrix[18]	N_2 matrix[18]	N_2 matrix[19]	Liquid He droplets[16]
Monomer									
$\nu_1 + \nu_4$(E), $\nu_3 + \nu_4$(E)	5026	5019	5047.5			5074.0, 5059.6	5043		
$\nu_1 + \nu_2(A_1)$, $\nu_3 + \nu_2$(E)	4415	4416	4450.1,4324.4			4466.7,4448.5*	4441,4319		
						4339.7,4319.2*			
ν_3(E)		/	3447.3	/		3465.4,	3440.7	/	3443.1
$\nu_1(A_1)$		3312	3345.4	3329		3364.2,	3330.6	3330	3335.8
$2\nu_4$(E)		3236	3238.8	3239			3234.8	3235	3238.7
$2\nu_4(A_1)$		3206		/			3234.8		3216.1
ν_4(E)	1618	1618	1638.9	1620		1644.7, 1643.1	1631	/	
$\nu_2(A_1)$	960	961	974.3	/		968.5, 960.9*	969.7	970	
Dimer									
$\nu_1 + \nu_4$(E), $\nu_3 + \nu_4$(E)	5012								
$\nu_1 + \nu_2(A_1)$, $\nu_1 + \nu_3$(E)	4432		4423,4306				4416		
ν_3(E)			3400.7	3421?, 3400	3422.3, 3400.7, 3393	3418.8	3402.4	3427?, 3402	3441.5,3431.2, 3423.1, 3420.4
$\nu_1(A_1)$			3310.8	3325, 3310	3325.3, 3310.8	3320.2	3312.1	3312	3326.2,3328.2, 3331.8, 3334.7
			3242.4	3242	3242.4, 3212.6	3253.3	3244.7	3244	
$2\nu_4$(E)									
$2\nu_4(A_1)$									3251
ν_4(E)			1631	1632	1631				
$\nu_2(A_1)$	970		999.8	1000	999.8		1003.6	1004 986	
Trimer									

$\nu_1 + \nu_4$(E), $\nu_3 + \nu_4$(E)						
$\nu_1 + \nu_2(A_1)$, $\nu_3 + \nu_2$(E)						
ν_3(E)	3391	3391	3413,3386		3391	3444.6,3433.3, 3403.0,3399.2
$\nu_1(A_1)$	3306	3304	3315, 3246	3310	3308	3316.5
	3236, 3212	3236, 3212	3242, 3219	3216,3240	~3230, ~3215	
$2\nu_4$(E)						3321.0
$2\nu_4(A_1)$						3256.5
ν_4(E)	1645	1645	1636	1013		
$\nu_2(A_1)$	1018	1018	1038		1014	
Multimer						
		3378			3384	
		3296				
		3228				
		3202				

*site splitting

Table 2. Assignment of the monomer and resulting oligomer absorption bands of ND_3 in LXe at 203 K and a comparison with previous literature investigations.

Assignment	Experiment	Literature	
	Liquid Xe 203 K	Ar matrix [18]	Ar matrix [20]
Monomer			
$\nu_1 + \nu_3$	4865		
$\nu_1 + \nu_4$(E), $\nu_3 + \nu_4$(E)	3724		
$\nu_1 + \nu_2(A_1)$, $\nu_3 + \nu_2$(E)	3321		
ν_3(E)	2545	2553	2548.5, 2543.8, 2527
$\nu_1(A_1)$	2406	2414	2410, 2373
$2\nu_4$(E)	/		2346.4
$2\nu_4(A_1)$	/		2340
ν_4(E)	1183	1190	1185
$\nu_2(A_1)$	770	760	781
Dimer			
$\nu_1 + \nu_4$(E), $\nu_3 + \nu_4$(E)			
$\nu_1 + \nu_2(A_1)$, $\nu_3 + \nu_2$(E)	3321		
ν_3(E)	2529	2527	
$\nu_1(A_1)$	2406	2410	
		2373	
$2\nu_4$(E)	2371		
$2\nu_4(A_1)$	2346		
ν_4(E)		1185	
$\nu_2(A_1)$		781	
Trimer			
$\nu_1 + \nu_4$(E), $\nu_3 + \nu_4$(E)			
$\nu_1 + \nu_2(A_1)$, $\nu_3 + \nu_2$(E)			
ν_3(E)	2541, 2519	2519	
$\nu_1(A_1)$	2405	2410(D+T)	
		2318, 2336	
$2\nu_4$(E)	2370		
$2\nu_4(A_1)$	2343		
ν_4(E)		1206	
$\nu_2(A_1)$		792	
Tetramer			
ν_3(E)	2505		

ACKNOWLEDGMENT

The authors acknowledge the Research Foundation Flanders, FWO, for an appointment of a PhD Fellowship (11C5814N) and for the financial help towards the purchase of spectroscopic equipment used in this study. The authors thank the Flemish Community for the financial support through the Special Research Fund (BOF). Yannick Geboes is thanked for valuable discussions.

REFERENCES

[1] W. Herrebout, Top. Curr. Chem., 358 (2015) 79-154.
[2] J.J.J. Dom, B.J. van der Veken, B. Michielsen, S. Jacobs, Z.F. Xue, S. Hesse, H.M. Loritz, M.A. Suhm, W.A. Herrebout, Phys. Chem. Chem. Phys., 13 (2011) 14142-14152.
[3] B. Michielsen, J.J.J. Dom, B.J. van der Veken, S. Hesse, M.A. Suhm, W.A. Herrebout, Phys. Chem. Chem. Phys., 14 (2012) 6469-6478.
[4] N. Nagels, Y. Geboes, B. Pinter, F. De Proft, W.A. Herrebout, Chem. Eur. J., 20 (2014) 8433-8443.
[5] D. Hauchecorne, R. Szostak, W.A. Herrebout, B.J. van der Veken, ChemPhysChem, 10 (2009) 2105-2115.
[6] D. Hauchecorne, B.J. van der Veken, A. Moiana, W.A. Herrebout, Chem. Phys., 374 (2010) 30-36.
[7] D. Hauchecorne, A. Moiana, B.J. van der Veken, W.A. Herrebout, Phys. Chem. Chem. Phys., 13 (2011) 10204-10213.
[8] Y. Geboes, N. Nagels, B. Pinter, F. De Proft, W.A. Herrebout, J. Phys. Chem. A, 119 (2015) 2502-2516.
[9] L.I. De Beuckeleer, W.A. Herrebout, Spectrochim. Acta A, 154 (2016) 89-97.
[10] W.A. Herrebout, S.M. Melikova, S.N. Delanoye, K.S. Rutkowski, D.N. Shchepkin, B.J. van der Veken, J. Phys. Chem. A, 109 (2005) 3038-3044.
[11] K.S. Rutkowski, W.A. Herrebout, S.M. Melikova, P. Rodziewicz, B.J. van der Veken, A. Koll, Spectrochim. Acta A, 61 (2005) 1595-1602.
[12] in MATLAB 8.3, The MathWorks Inc., Natick, MA, USA, 2014.
[13] B.J. van der Veken, F.R. De Munck, J. Chem. Phys., 97 (1992) 3060-3071.
[14] B.J. van der Veken, J. Phys. Chem., 100 (1996) 17436-17438.
[15] G. Schwarz, The Annals of Statistics, 6 (1978) 461-464.
[16] M.N. Slipchenko, B.G. Sartakov, A.F. Vilesov, S.S. Xantheas, J. Phys. Chem. A, 111 (2007) 7460-7471.
[17] F.P. Reding, D.F. Hornig, J. Chem. Phys., 19 (1951) 594.
[18] S. Suzer, L. Andrews, J. Chem. Phys., 87 (1987) 5131-5140.
[19] A.J. Barnes, J. Mol. Struct., 237 (1990) 19-32.
[20] J.P. Perchard, R.B. Bohn, L. Andrews, J. Phys. Chem., 95 (1991) 2707-2712.

Highlights

- Self-association of NH_3 and ND_3 is observed in the infrared spectra of cryosolutions with liquid xenon.

- Least-squares fitting of polynomials to the recorded data allows us to resolve spectral regions with overlapping absorbance bands.

- Least-squares fitting of polynomials yields accurate information on monomer, dimer, trimer and tetramer species present in the solutions.

- The least-squares fitting method shows an added value towards other methods often used.